Simulating Effects of Probe Placement on Calibration Accuracy using TRL

Tyler Angell, School of Electrical, Computer and Energy Engineering, Arizona State University, Tempe, AZ USA

***Abstract*— The objective of this research is to simulate the effects of probe placement on calibration accuracy using the TRL calibration. Using HFSS, coplanar standards were designed and simulated on silicon between 300 GHz and 489 GHz. In Python, Gaussian noise was added to the shift the reference planes of the standard measurements in order to simulate probe placement error. Python was also used to code the TRL algorithm. Taking 100 runs allowed for the characterization of the effects of this simulated probe placement error. This method showed the effect of probe positioning error on the measurement of real loads.**

***Index Terms*—Calibration accuracy, calibration standards, Thru-Reflect-Line (TRL), coplanar waveguide (CPW), terahertz (THz), systematic error, probe placement accuracy, displacement error.**

I. Introduction

CALIBRATION of network analyzers is important to make accurate measurements by mitigating systematic errors. It effectively reduces the effect of systematic errors using standard measurements and error correcting algorithms. However, calibration does not remove the presence of all errors in the system. Due to the nature of the calibration, in die-probing measurements there is unavoidable mechanical error in probe placement [1]. The algorithm used in this investigation is the Thru-Reflect-Line or TRL. The TRL calibration utilizes three standards: a zero-length thru (T), a high-reflect open or short (R), and a longer thru or line (L). This algorithm was chosen for its ease of manufacturability, superior accuracy for non-coaxial applications, and flexibility of only needing to know the impedance and approximate electrical length of the line standard [2] Measuring these standards allow for the calculation of the calibrated value (without the presence of systematic errors) of the device under test (DUT) [3]. Due to the mechanics of the physical TRL calibration in probe measurements, it is prone to error due to the mechanical uncertainty of probe re-positioning which can lead to significant errors when measuring at sub-THz frequencies and higher [4]. Using 3D EM modeling and computational software, this research simulates the mechanical uncertainty present from probe placement on pads in one dimension when measuring the standards and DUT, and it characterizes the error introduced on the actual measurements.

II. Material and Methods

To investigate how network analyzers deal with the presence of errors, this work will rely upon well-known network analyzer calibration techniques such as TRL. To simulate these, the use of computational software (HFSS and Python) will be used. Although there are limitations to this study since there is not a physical system, 3D EM software allows for the modeling of standards to represent the physical system. Using Python, errors representing mechanical probe placement error can be artificially introduced. The measured values of the standards will be perturbed by noise with a known mean and standard deviation, and this can be used to map to some standard deviation away from a given load.

A. Theory: Determining the Value of the DUT

Using the TRL algorithm from [3] allows for the calculation of the de-embedded device parameters. Once these parameters are known, further analysis allows for the determination of the impedance of the device under test. In an ABCD matrix for a series load this impedance corresponds to B. However, this impedance value may not accurately represent the impedance of the device under test due to intrinsic capacitance. This capacitance can be modeled as a capacitor in parallel with the load. For this study using coplanar waveguides, the effects of this intrinsic capacitance were measured and accounted for by measuring a specific open (standard with the DUT removed); knowing the measured value of the load and the capacitance of the open, the actual impedance of the load can be determined as shown using (1a) and (1b).

$$Z = Z_L || Z_C \tag{1a}$$

$$Z_L = \frac{Z * Z_C}{Z_C - Z} \tag{1b}$$

B. Simulating Probe Placement Error

In order to simulate probe placement error, noise was artificially introduced in the measurements. It is assumed that the probe placement error could be approximated using a Gaussian distribution. According to [5], current probing technologies allow for sub-micron placement accuracy. This lead to the choice of mean of 0 µm and a standard deviation of 1 µm for the Gaussian distribution. This noise was able to be

applied to the results as a shift in reference planes on both ports for each standard as shown in (2) from [3]. Since, $\theta = \beta\ell$, the noise can be applied to length ℓ which represents the displacement of the probe from the target reference plane in one dimension.

$$[S'] = \begin{bmatrix} e^{-j\theta_1} & & 0 \\ & e^{-j\theta_2} & \\ & & \ddots \\ 0 & & e^{-j\theta_N} \end{bmatrix} [S] \begin{bmatrix} e^{-j\theta_1} & & 0 \\ & e^{-j\theta_2} & \\ & & \ddots \\ 0 & & e^{-j\theta_N} \end{bmatrix} \quad (2)$$

C. *Building Models and Implementation of Noise*

Coplanar models were built using HFSS. The TRL standards, a DUT, and an open with the DUT removed were built on silicon for the frequency range of 300 GHz to 489 GHz. The conductor was a sheet and made of PEC. The spacing was 3 µm and the track width was 5 µm. The DUT was a 5 µm by 5 µm square sheet set as an impedance boundary. Impedances of 50 Ω, 500 Ω, and 5K Ω were used. The data was taken from these models and processed using Python.

The TRL algorithm was programmed in Python. The noise was introduced using a Gaussian random number generator and applied using (2) for each of the S-Parameters at each frequency. Thus, a total of 10 random errors were introduced: one for each port for each of the TRL standards, DUT, and open. Using the methods described previously, the impedance was determined at each frequency. For this study, 100 runs of this process were used to characterize the effects of probe placement error on the measurement of the load.

III. Experimental Results

To ease in the explanation of the results, the results of the 500 Ω DUT will be used as an example. The control for this experiment was the actual impedance without noise. The results for the real impedance of the 500 Ω DUT are shown in Fig 1. This plot shows the load with and without the intrinsic capacitance in order to see the effects of the capacitance. Fig. 1. shows the effect of the intrinsic capacitance on the load and how it distorts the measurement of the actual load. These effects from the intrinsic capacitor become greater as the real load increases since more of the current is forced through the capacitor. Since the impedance without the intrinsic capacitance is the value of interest for this research, this data will be used going forward. The average value for the real part of this load was determined to be 494.32 Ω. Table I shows average of the real and imaginary impedance across the frequency band for the three loads.

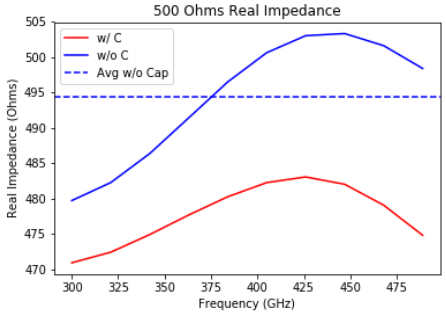

Fig. 1. Real impedance of 500 Ω DUT with and without intrinsic capacitance for comparison. These are the values before adding simulated probe placement error.

TABLE I
Average Impedance without Perturbation

DUT		Impedance
50 Ω	Re	49.96 Ω
	Im	7.742 Ω
500 Ω	Re	494.32 Ω
	Im	39.32 Ω
5K Ω	Re	5859.91 Ω
	Im	-0.8887 Ω

Incorporating perturbations on each port for each standard for 100 runs produces a noisy plot. By taking the mean and standard deviation of the noisy values at each frequency, the characteristics of the noise distribution can be captured at each frequency as shown in Fig. 2. for the real impedance of the 500 Ω DUT. This plot shows average (black horizontal line) and standard deviation in the thicker error bar; the minimum and maximum values are shown at the endpoints of the thinner error bar. The control data from the noiseless run was included for comparison. It is evident from this plot how the simulated probe placement error (noise) causes deviation from the actual value.

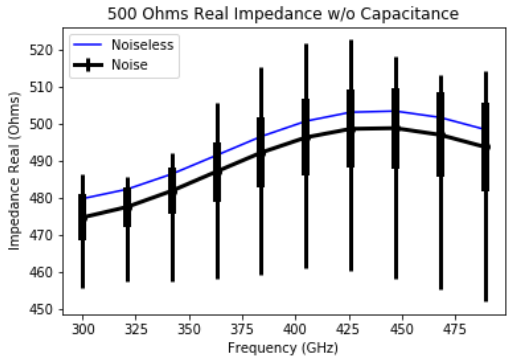

Fig. 2. Noise distribution (black) of real impedance of 500 Ω DUT with thick error bars showing standard deviation, thin error bars showing minimum and maximum values, and average along the black line. The blue line shows the real impedance without added noise.

A histogram for the 500 Ω DUT was plotted at 300 GHz for the 100 runs as shown in Fig. 3(a). It is difficult to determine the distribution off of a few samples, so the number of samples was increased to 1000. The Gaussian noise applied to the standards resulted in what appears to be a Gaussian distribution for the 500 Ω DUT as shown in Fig. 3(b). which is to be expected.

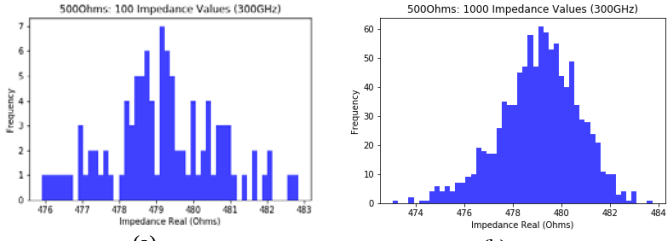

(a) (b)

Fig. 3. Histogram for the 500 Ω DUT at 300 GHz for (a) 100 runs and (b) 1000 runs.

Taking the average of the average values and the square root of the average variances (standard deviation) allowed for the characterization across the frequency band. These values are

shown in Table IIA on the left column. Using these generalized metrics, maximum percent error can be calculated in relation to the average value of the load without noise. Taking the example of the 500 Ω DUT, at one standard deviation, the maximum percent error between the average of the load with noise and the actual load without noise was 0.69% as seen in (3). For reference, a percent error of 1% on a 500 Ω load would be ±5 Ω. The maximum percent errors were calculated for the real and imaginary parts of all three noisy loads at one, two, and three standard deviations away from the load without noise. What this table reveals is that probe positioning error with a standard deviation of 1 µm from the target reference plane results in less than 1 percent average error at one standard deviation away from the mean of the perturbed measurements. The percent errors on the imaginary part of the load were much greater, and this is due to the greater variance and large standard deviation in proportion to the mean. However, the cause is uncertain for the greater variance relative to the mean for the imaginary component.

$$\left|\frac{(493.68\pm 2.77\Omega)-(494.32\Omega)}{494.32\Omega}\right| * 100 = 0.43\% \; or \; 0.69\% \quad (3a)$$

$$\left|\frac{(493.68-2.77\Omega)-(494.32\Omega)}{494.32\Omega}\right| * 100 = 0.69\% \quad (3b)$$

TABLE IIA
MAXIMUM PERCENT ERROR FOR STD. DEV. OF DISPLACEMENT AT 1 µM

			Percent Error from Load (noiseless)		
			1σ (%)	2σ (%)	3σ (%)
50 Ω	Re	µ=49.84, σ= 0.29	0.72	1.30	1.89
	Im	µ=10.73, σ= 2.52	71.22	103.82	136.43
500 Ω	Re	µ=493.68, σ= 2.77	0.69	1.25	1.81
	Im	µ=49.92, σ= 2.26	32.72	38.46	44.21
5K Ω	Re	µ=5851.24, σ= 46.39	0.94	1.73	2.52
	Im	µ=-33.88, σ= 85.61	13346.52	22979.75	32612.98

Further simulations were performed, but the standard deviation of the noise was extended to 2 µm. The following Table IIB was produced. The errors on the real part of the loads were still relatively small, and the errors on the imaginary parts remained large. Similar results can be seen for Table IIC with the standard deviation of the displacement extended to 3 µm.

TABLE IIB
MAXIMUM PERCENT ERROR FOR STD. DEV. OF DISPLACEMENT AT 2 µM

			Percent Error from Load (noiseless)		
			1σ (%)	2σ (%)	3σ (%)
50 Ω	Re	µ=49.68, σ= 0.61	1.67	2.90	4.13
	Im	µ=10.86, σ= 5.04	105.44	170.52	235.61
500 Ω	Re	µ=492.14, σ= 5.80	1.61	2.78	3.96
	Im	µ=49.88, σ= 4.59	38.55	50.23	61.92
5K Ω	Re	µ=5831.15, σ= 95.41	2.11	3.74	5.37
	Im	µ=-32.93, σ= 180.00	23860.15	44114.51	64368.87

TABLE IIC
MAXIMUM PERCENT ERROR FOR STD. DEV. OF DISPLACEMENT AT 3 µM

			Percent Error from Load (noiseless)		
			1σ (%)	2σ (%)	3σ (%)
50 Ω	Re	(µ=49.43 σ= 0.98)	2.91	4.89	6.86
	Im	(µ=10.97 σ= 7.52)	138.90	236.10	333.31
500 Ω	Re	(µ=489.72 σ= 9.32)	2.81	4.70	6.58
	Im	(µ=49.79 σ= 7.05)	44.57	62.50	80.43
5K Ω	Re	(µ=5797.59 σ= 150.40)	3.63	6.19	8.76
	Im	(µ=-26.25 σ= 297.61)	36343.76	69832.85	103321.94

Using the real part of the 500 Ω DUT, the average percent error was tracked over the standard deviation of displacement as shown in Fig. 4. It appears that the error is exponential in relation to the displacement.

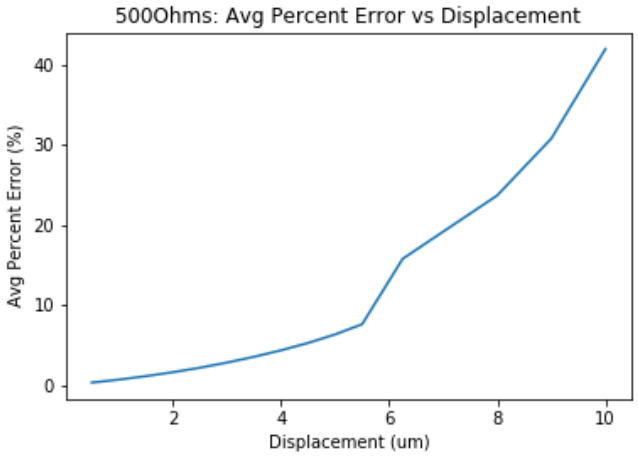

Fig. 4. Average percent error tracked over the standard deviation of displacement.

IV. CONCLUSION

This research has focused on the effects of probe placement on calibration accuracy using the TRL calibration. It was found that probe positioning error with a standard deviation of 1 µm from the target reference plane results in less than 1 percent error at one standard deviation away from the mean of the perturbed measurements. For a standard deviation of 2 µm from the target reference plane there was less than 2.2 percent error at one standard deviation away from the mean of the perturbed measurements. For a standard deviation of 3 µm from the target reference plane there was less than 3.7 percent error at one standard deviation away from the mean of the perturbed measurements. Tracking the average percent error over displacement, it appears that the percent error increases exponentially as a function of displacement.

Future work could be done to determine the reasons why the perturbations caused more variance in the imaginary part of the load. Another area that may provide valuable insight is to investigate complex loads and determine whether the imaginary part of the loads can be successfully recovered. Finally, this research could be implemented in physical standards and can be compared to the simulated results.

REFERENCES

[1] T. Reck, L. Chen, C. Zhang, C. Groppi, H. Xu, A. Arsenovic, S. Barker, A. Lichtenberger, R. Weikle, "Calibration accuracy of a 625 GHz on-wafer probe", *76th ARFTG Microw. Meas. Conf. Dig.*, 2010-Dec.

[2] Advanced Calibration Techniques for Vector Network Analyzers. (2018). 2nd ed. [ebook] Agilent Technologies. Available at: http://anlage.umd.edu/Agilent_Advanced_VNA_calibration.pdf [Accessed 23 Apr. 2018].

[3] Pozar, D. (2012). *Microwave engineering*. Hoboken, NJ: Wiley.

[4] Chien, J. and Niknejad, A. (2017). *Advanced High-Frequency Measurement Techniques for Electrical and Biological Characterization in CMOS*. [online] Berkeley: University of California at Berkeley, p.1. Available at: https://www2.eecs.berkeley.edu/Pubs/TechRpts/2017/EECS-2017-9.pdf [Accessed 23 Apr. 2018].

[5] FormFactor. (2018). *Cascade SUMMIT200*. [online] Available at: https://www.formfactor.com/product/probe-systems/200-mm-systems/summit200/ [Accessed 27 Apr. 2018].